# Microstructure and Dielectric Behavior of Ytterbium Doped BaZr$_{0.1}$Ti$_{0.9}$O$_3$ Ceramics

*Yuanliang Li[a]\*, Zhimin Cui[a], Rongli Sang[a], Xuegang Ma[a]*

*[a] Hebei Provincial Key Laboratory of Inorganic Nonmetallic Materials, North China University of Science and Technology, Tangshan 063009, China*

BaZr$_{0.1}$Ti$_{0.9}$O$_3$ ceramics of perovskite structure are prepared by solid state reaction method with addition of x Yb$_2$O$_3$ (x= 0.0, 0.1, 0.3, 0.5 and 0.7 mol%), respectively, and their dielectric properties are investigated. Room temperature X-ray diffraction study suggested that the compositions have a single phase with a perovskite structure. A small decrease in the grain size is observed with an increase in the Yb content. The bulk density increased with increasing the Yb content for the samples sintered at 1250 ºC, and the bulk densities show the maximal value for the samples sintered at 1280 ºC, 1300 ºC and 1330 ºC. The dielectric constant can reach to 4500 or more for the sample sintered at 1300 ºC, and the variation of dielectric loss with temperature is more stable for Yb$_2$O$_3$-doped BZT10 ceramics, which proves that Yb$_2$O$_3$ doping has a great influence on the dielectric properties in BZT10 ceramics. With the increase of Yb$_2$O$_3$ content, $T_c$ rises at first, and when x exceeds 0.1 mol%, $T_c$ shifts towards to lower temperature with the Yb$_2$O$_3$ concentration increasing.

**Keywords:** *Ceramics; Dielectric properties; Ferroelectrics; Solid state reaction*

## 1. Introduction

A large number of BaTiO$_3$-based (BT) solid solutions have been studied in the last years due to environmental concerns which are driving the exploration for new Pb-free piezo/ferroelectric materials with superior performances[1,2]. BaTiO$_3$-based ceramics is widely used ferroelectrics in the microelectronic industry, especially as piezoelectric actuators, dielectric material in multilayer ceramic capacitors (MLCC), pyroelectric detectors, electroluminescent panels, embedded capacitance in printed circuit boards and positive temperature coefficient of resistivity (PTCR) sensors, et al.[3-5] The solid solution of BaZr$_x$Ti$_{1-x}$O$_3$ (BZT) is one of the most important compositions for dielectrics in multilayer ceramic capacitors[6], because the ion Zr has higher chemical stability than the ion Ti[7], and the high permittivity of the BaTiO$_3$ ceramic is increased more by the addition of zirconium. In particular, modified (BZT) ceramics receives considerable attention due to their tunable behavior and better electrical properties[8,9], and the nature of the ferroelectric phase transition of BZT bulk ceramics is known to strongly change with the Zr content increasing. For lower Zr concentrations (0< $x$ < 0.10), BZT behaves like a normal ferroelectric material. At higher Zr content (0.10 ≤ $x$ ≤ 0.42), bulk BZT ceramics show a broad dielectric constant–temperature ($\varepsilon$–$T$) curve near $T_c$, which may be caused by the inhomogeneous distribution of Zr ions on Ti sites and mechanical stress in the grains, and antiferroelectric properties for Zr-rich compositions is observed. The system exhibits a pinched phase transition with increasing Zr concentration (at $x \approx 0.15$), the three phase transitions are merged into one broad peak.

Trivalent rare earth cations are widely used to modify the BaTiO$_3$ properties because of their moderate ionic radii and ability to substitute both A and B sites[10-12]. The ionic radius of the rare earth ions are in between that of Ba$^{2+}$ ion and Ti$^{4+}$ ions. The influence of rare earth dopant on the dielectric properties of BaTiO$_3$-based ceramics has been widely researched. However, the doping of Ytterbium in BZT ceramics is rarely found in the literature. In the present study, BZT + x Yb$_2$O$_3$ ceramics (x= 0.0, 0.1, 0.3, 0.5 and 0.7 mol%) is prepared in an ambient atmosphere by a conventional solid state reaction technique, and the effect of substitution of different Yb concentration on the structure and dielectric properties of BZT ceramics has been investigated.

## 2. Experimental Procedure

In the present experiment, BaZr$_{0.1}$Ti$_{0.9}$O$_3$ ceramics (BZT10) has been chosen as the ground component. The ceramics were prepared by the two-stage method using starting chemicals of TiO$_2$ (AR, China), ZrO$_2$ (AR, China), BaCO$_3$ (AR, China) and Yb$_2$O$_3$ (99.99%, China). Firstly, to disperse the precursor, the mixtures based on the composition of BZT10 were ball-milled for 6 h with zirconia media in ethanol (Model QM- QX4 planetary ball mill, China). After drying, the powders were thermally treated at 1080 ºC for 2 h, producing a precursor to which it was added the Yb$_2$O$_3$. Secondly, the powders were re-milled for 12 h to mix the mixtures well. The mixtures were then dried at 120 °C, granulated (with polyvinyl alcohol as binder), pressed into pellets (Φ×$d$ = 13.20×2.00 mm$^2$) at 100 MPa, and then sintered at 1,250°C, 1,280, 1,300 °C and 1,330 °C for 2 h

\* e-mail: lylll2004@126.com

in the air. The thickness of the obtained samples is about 1.9 mm. Both sides of the specimens for dielectric property measurements were screened with Ag electrode paste, and then fired at 470 °C for 10 min.

Phase compositions of the ceramics were investigated using X-ray powder diffraction patterns at room temperature (XRD, RIGAKU D/MAX 2500V/PC, Japan) with Cu Kα radition. The powder diffraction diagrams were obtained in the $10^\circ \leq 2\theta \leq 120^\circ$ angular range with a step of $0.02^\circ$ and a counting time of 5 s per step. The as-obtained PXRD were analyzed by Rietveld method using Fullprof software[13]. The microstructures of the samples were observed by field emission scanning electron microscopy (SEM, Hitachi s4800). Raman spectra were acquired using a DXR Raman microscope by Thermo Scientific Nicolet (USA) using a green laser (532 nm) and power of 3 mW under an objective of 50 magnification. The room resistivity was measured by high resistance meter (Model ZC36 high resistance meter, China), and the room resistivity of all the samples is above $1.0 \times 10^{11}$ Ω·m, so, the materials in our experimental don't process on semi-conductivity. Capacitance and dielectric loss were measured over 20 °C to 125 °C using a capacitance apparatus (Model YY 281 automatic LCR Meter 4225, China) at 1 kHz.

## 3. Results and discussion

### 3.1 The effect of Yb$_2$O$_3$ on microstructure

The XRD patterns of the samples with different amounts of Yb$_2$O$_3$ contents sintered at 1,300 °C for 2 h are shown in Figure 1. It is observed that BZT10 ceramics processes distinct peaks (100), (110), (111) and (002), indicating that as-prepared samples consist of a single phase with a perovskite structure. Structural study as Rietveld refinement of the X-ray diffraction pattern as typical representative x Yb$_2$O$_3$ + BZT10 ceramics (x=0) illustrated in Figure 2[14]. After a successful refinement of the diffraction data, all the obtained parameters like, lattice parameters, and other figure of merit parameters are listed in Table 1. Obviously, the ceramics exhibit tetragonal structure with space group *P4mm* when x ≤ 0.5, and the sample exhibits cubic structure with space group *R3c* when x = 0.7.

For the sample doped with 0.5 mol% Yb$_2$O$_3$, the XRD patterns with different sintering temperature are shown in Figure 3. From the figure, it can be seen that the diffraction peaks (100); (210); (220) are widened for the samples sintered at 1300 ℃ and 1330 ℃. In order to check the structure changes, an analysis by Raman spectroscopy was employed for the samples sintered at 1300 ℃ and 1330 ℃, and the results can be seen in Figure 4. For the sample sintered at 1330 ℃, the frequency of E(TO) shifts to lower direction, $T_c$ should decrease, so, the crystal structure may be still cubic phase in the room temperature[15].
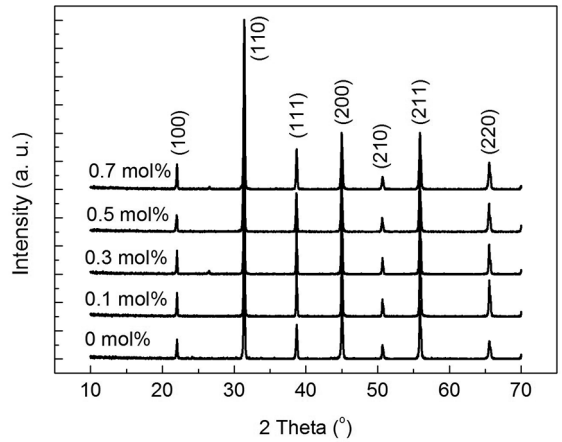


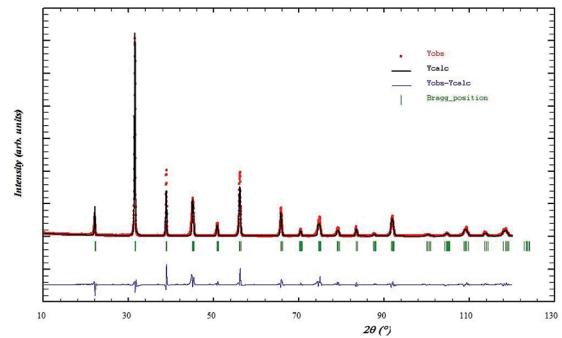**Figure 1:** XRD patterns of BZT10 + x Yb$_2$O$_3$ ceramics.



**Figure 2:** The Rietveld plot of the X-ray diffraction pattern of BaZr$_{0.1}$Ti$_{0.9}$O$_3$ ceramics

Figure 5 shows the bulk densities of the studied samples measured by the Archimedes principle sintered at different temperatures. Very interestingly, the measured bulk density increased with increasing the Yb content for the samples sintered at 1250 °C, however, when the concentration of Yb$_2$O$_3$ content is 0.5 mol%, the measured bulk densities show the maximal value for the samples sintered at 1280 °C, 1300°C and 1330°C. The SEM micrographs of the investigated BZT10 ceramics presented in Figure 6 show dense and homogeneous microstructures, a small decrease in the grain size is observed with an increase in the Yb content, however, the increase is less apparent.

### 3.2 The effect of Yb$_2$O$_3$ on dielectric behavior

Figure 7 shows influence of Yb$^{3+}$ content on dielectric constants of the samples sintered at 1250 ℃, 1280 ℃, 1300 ℃ and 1330 ℃ for 2 h, respectively. As can be seen from Figure 7, for the samples sintered at 1250 ℃ for 1280 ℃, the dielectric constant decreases slowly at first and then increases, and for the samples sintered at 1300 ℃ and 1330 ℃, both the dielectric constant reached the maximum when the Yb$_2$O$_3$ concentration is 0.5 mol%, and the dielectric constant can be up to 4500 or more for the sample sintered
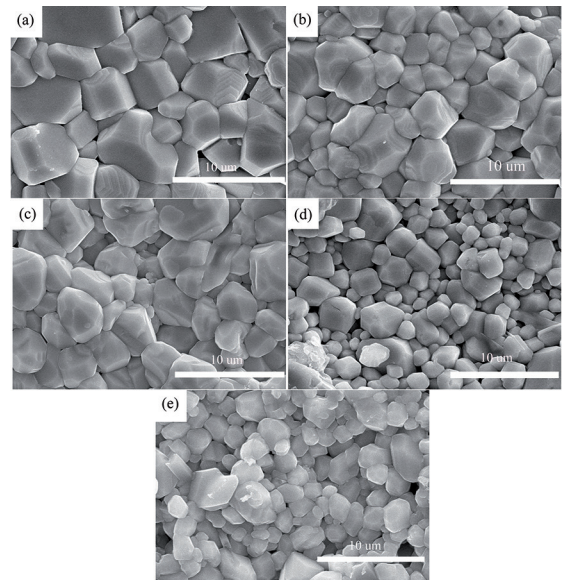
**Table 1:** The merit for x Yb$_2$O$_3$ + BZT$_{10}$ ceramics

| x (mol%) | Refined parameters | | | Lattice parameters (nm) | | | c/a |
|---|---|---|---|---|---|---|---|
| | $R_p$ | $R_{wp}$ | $R_{exp}$ | a | b | c | |
| 0.0 | 13.2 | 15.3 | 4.03 | 0.41652 | 0.41652 | 0.42021 | 1.009 |
| 0.1 | 12.1 | 13.7 | 3.88 | 0.41476 | 0.41476 | 0.41932 | 1.011 |
| 0.3 | 12.8 | 14.1 | 3.76 | 0.41498 | 0.41498 | 0.41747 | 1.006 |
| 0.5 | 11.6 | 13.5 | 3.67 | 0.41523 | 0.41523 | 0.41689 | 1.004 |
| 0.7 | 13.1 | 14.4 | 3.94 | 0.41588 | 0.41588 | 0.41588 | 1 |
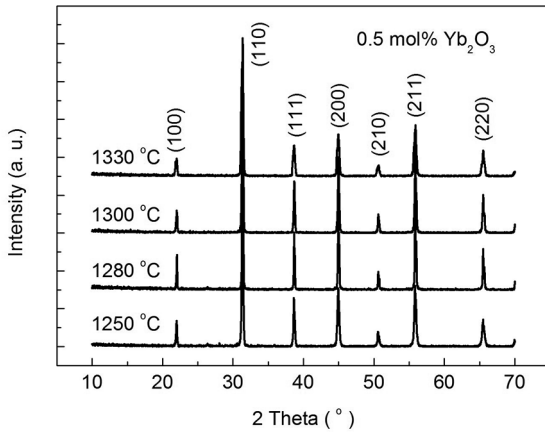


**Figure 3:** XRD patterns of BZT10 + 0.5 mol% Yb$_2$O$_3$ ceramics at various sintering temperature.
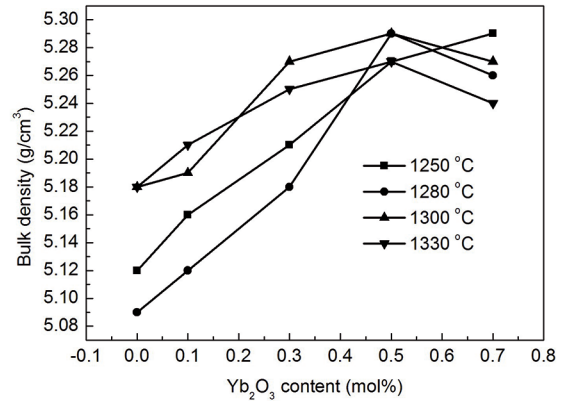


**Figure 5:** Bulk density of BZT10 + x Yb$_2$O$_3$ ceramics sintered at different temperature.
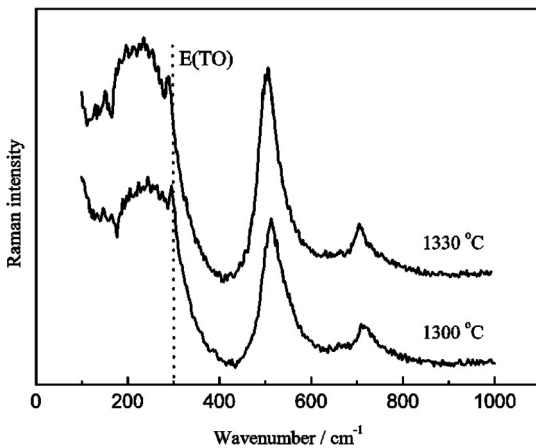


**Figure 4:** Room temperature depolarized Raman spectra for the samples.



**Figure 6:** Surface SEM images of BZT10 ceramics sintered at 1300 °C/2 h (a) 0 mol%, (b) 0.1 mol%, (c) 0.3 mol%, (d) 0.5 mol%, (e) 0.7 mol%.

at 1300 °C, with the Yb$_2$O$_3$ concentration further increasing, the dielectric constant decreases, which may be related with change of the crystal structure. The results show that Yb$_2$O$_3$ doping has a great influence on the dielectric constant in BZT10 ceramics.

The temperature dependence of the dielectric constants for BZT10 + x Yb$_2$O$_3$ ceramics sintered at 1300 °C for 2 h is illustrated in Figure 8. Due to the addition of Yb$_2$O$_3$, the dielectric peak is remarkably broadened, which is a

characteristic of diffuse phase transition (DPT) [16]. With the increase of Yb$_2$O$_3$ content, $T_c$ rises slightly from 76 °C for the undoped Yb$_2$O$_3$ sample to 88 °C for the 0.1 mol% Yb$_2$O$_3$ doped sample in the beginning, when x exceeds 0.1 mol%, $T_c$ shifts towards the low temperature with Yb$_2$O$_3$
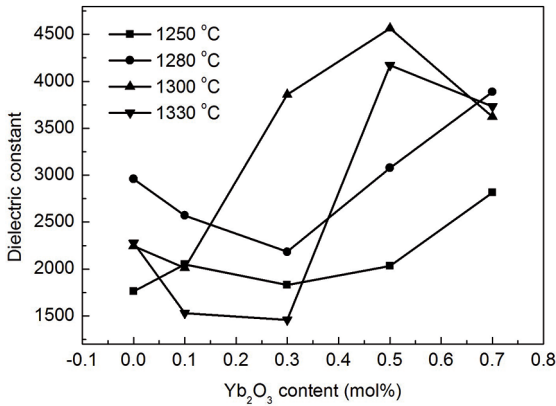
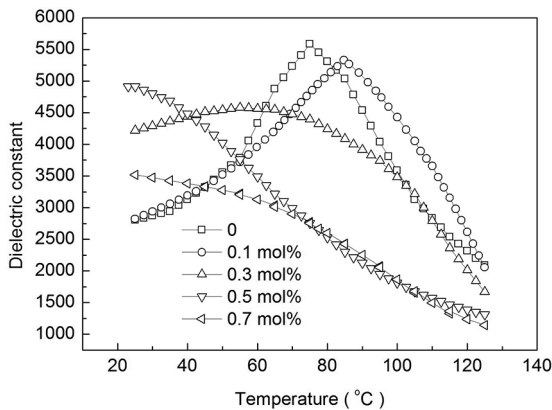**Figure 7:** Dielectric constant of BZT10 + x Yb$_2$O$_3$ ceramics sintered at different temperature.



**Figure 8:** Temperature dependence of dielectric constant of BZT10 + x Yb$_2$O$_3$ ceramics sintered at 1300 °C/2 h



**Figure 9:** Temperature dependence of dielectric constant of BZT10 + 0.5 mol% Yb$_2$O$_3$ ceramics sintered at different temperature.

increasing. It is reported that the transition temperature $T_c$ decreases as the grain size decreases. The effect of grain size originates from the higher surface tension in smaller grains, which acts in the same manner as hydrostatic pressure thus decreasing the Curie point[17]. In addition, the force experienced by the atoms and ions in the vicinity of, or far from, the surface of grain are not similar. For smaller grain sizes however, the superficial layers of the grains represent a significant fraction and may dominate the structural and the dielectric measurement[18]. Table 1 also shows the tetragonality (*c*/*a* ratio), and the *c*/*a* ratio is according to the shifting of $T_c$[7]. From Figure 8, it can also be seen that the maximum dielectric constant ($\varepsilon_m$) for the undoped Yb$_2$O$_3$ sample is highest, the maximum dielectric constant ($\varepsilon_m$) of Yb-doped BZT10 ceramics decreases with the increasing of Yb$_2$O$_3$ content, and the maximum dielectric constant ($\varepsilon_m$) for the 0.7 mol% Yb$_2$O$_3$ doped sample is lowest. The reason for the decrease of the maximum dielectric constant is that the grain size decreases with the increasing of Yb$_2$O$_3$ content.

Figure 9 shows temperature dependence of dielectric constant of BZT10 + 0.5 mol% Yb$_2$O$_3$ ceramics sintered at different temperature. As for the transition temperature
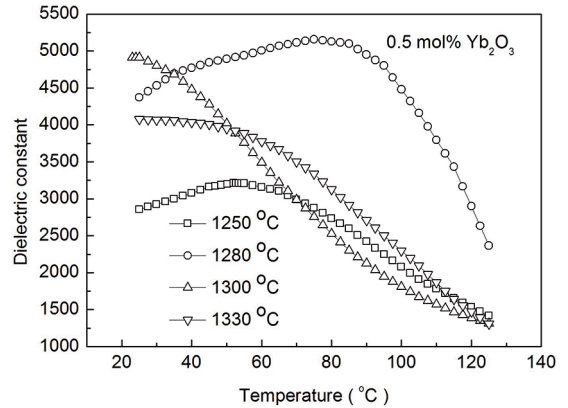
$T_c$, it rises from 55 °C for the sample sintered at 1250 °C to 82 °C for the sample sintered at 1280 °C in the beginning, and then $T_c$ shifts towards the lower temperature with the sintering temperature increasing, for the sample sintered at 1330 °C, we don't obtain it's $T_c$, demonstrating its $T_c$ is under the room temperature. In terms of $T_c$ (phase transition) in perovskite structure, the phase transition is related with the structure crystalline, that is, the tetragonal structure is stable when the temperature is lower than $T_c$, on the contrary, the cubic structure is stable when the temperature is above $T_c$. In the same time, the sample sintered at 1280 °C possesses the highest maximum dielectric constant ($\varepsilon_m$). That may be caused by the relatively large ionic radius of the B ion which enhances the thermal stability of the BO$_6$ octahedral, when compared to Ti or Zr. Also, the packing density of the BO$_6$ octahedral will be determined by the size of the B ion. Larger B ions give more closely packed octahedral, which are, therefore, more stable[19].

Temperature dependence of dielectric loss of BZT10 + x Yb$_2$O$_3$ ceramics is shown in Figure 10. Obviously, the variation of dielectric loss with temperature is more stable for Yb$_2$O$_3$-doped BZT10 ceramics. Therefore, in the terms of dielectric constant, dielectric loss and temperature stability for dielectric loss, the trace amount of Yb$^{3+}$ doping could influence the dielectric properties remarkably.

## 3. Conclusions

By using BaCO$_3$, ZrO$_2$ and TiO$_2$ as raw materials, BaZr$_{0.1}$Ti$_{0.9}$O$_3$ (BZT10) ceramics were prepared by the solid-state reaction, the effects of Yb$_2$O$_3$ doping amount and sintering temperature on the dielectric properties of BZT10 ceramics were investigated. Room temperature X-ray diffraction study suggested that the compositions have a single phase with a perovskite structure. Owing to the Yb$^{3+}$ doping, a small decrease in the grain size is observed with an increase in the Yb$_2$O$_3$ content, the bulk density increases with increasing the Yb content for the samples sintered at 1250 °C, and the bulk
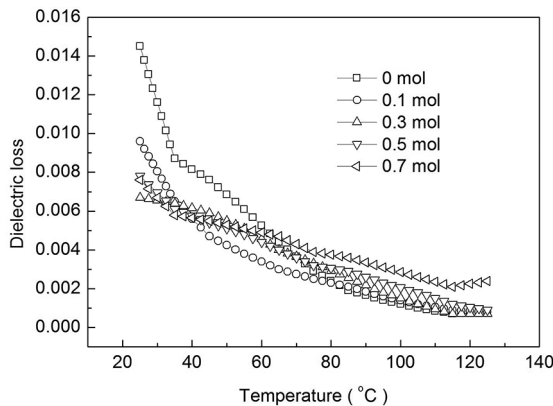
**Figure 10:** Temperature dependence of dielectric loss of BZT10 + x $Yb_2O_3$ ceramics sintered at 1300 ℃/2 h

densities show the maximal value for the samples sintered at 1280 °C, 1300°C and 1330°C. The room dielectric constant can reach to 4500 or more for the sample with 0.5mol% sintered at 1300 ℃, and the variation of dielectric loss with temperature is more stable for $Yb_2O_3$-doped BZT10 ceramics, with the increase of $Yb_2O_3$ content, $T_c$ rises at first, and when x exceeds 0.1 mol%, $T_c$ shifts towards to lower temperature with the $Yb_2O_3$ concentration increasing, which proves that $Yb_2O_3$ doping has a great influence on the dielectric properties in BZT10 ceramics. $T_c$ rises from 55 ℃ for the sample sintered at 1250 ℃ to 82 ℃ for the sample sintered at 1280 ℃ in the beginning, and then $T_c$ shifts towards the lower temperature with the sintering temperature increasing.

## 4. Acknowledgements:

## 5. References

1. Anthoniappen J, Tu CS, Chen PY, Chen CS, Chiu SJ, Lee HY, et al. Structural phase stability and electric field induced relaxor–ferroelectric phase transition in $(1-x)(Bi_{0.5}Na_{0.5})TiO_3-xBaTiO_3$ ceramics. *Journal of Alloys and Compounds*. 2015;618:120-126.

2. Rani A, Kolte J, Vadla SS, Gopalan P. Structural, electrical, magnetic and magnetoelectric properties of Fe doped $BaTiO_3$ ceramics. *Ceramics International*. 2016;42(7):8010-8016.

3. Huo W, Qu Y. Effects of $Bi_{1/2}Na_{1/2}TiO_3$ on the Curie temperature and the PTC effects of $BaTiO_3$-based positive temperature coefficient ceramics. *Sensors and Actuators A: Physical*. 2006;128(2):265-269.

4. Kang JH, Cha HM, Jung YG, Paik U. Crack suppression and residual stress in $BaTiO_3$ based Ni-MLCCs of Y5V specification through post-process. *Journal of Materials Processing Technology*. 2008;205(1-3):160-167.

5. Cho SD, Lee JY, Hyun JG, Paik KW. Study on epoxy/$BaTiO_3$ composite embedded capacitor films (ECFs) for organic substrate applications. *Materials Science and Engineering: B*. 2004;110(3):233-239.

6. Chiang CS, Lee YC, Shiao FT, Lee WH, Hennings D. Effect of $TiO_2$ doped Ni electrodes on the dielectric properties and microstructures of $(Ba_{0.96}Ca_{0.04})(Ti_{0.85}Zr_{0.15})O_3$ multilayer ceramic capacitors. *Journal of the European Ceramic Society*. 2012;32(4):865-873.

7. Shan D, Qu YF, Song JJ. Dielectric properties and substitution preference of yttrium doped barium zirconium titanate ceramics. *Solid State Communications*. 2007;141(2):65-68.

8. Mahajan S, Haridas D, Sreenivas K, Thakur OP, Prakash C. Enhancement in electro-strain behavior by $La^{3+}$ substitution in lead free $BaZr_{0.05}Ti_{0.95}O_3$ ceramics. *Materials Letters*. 2013;97:40-43.

9. Ostos C, Martínez-Sarrión ML, Mestres L, Delgado E, Prieto P. The influence of *A*-site rare-earth for barium substitution on the chemical structure and ferroelectric properties of BZT thin films. *Journal of Solid State Chemistry*. 2009;182(10):2620-2625.

10. Gong H, Wang X, Zhang S, Li L. Synergistic effect of rare-earth elements on the dielectric properties and reliability of $BaTiO_3$-based ceramics for multilayer ceramic capacitors. *Materials Research Bulletin*. 2016;73:233-239.

11. Li Y, Wang R, Ma X. Dielectric behavior of samarium-doped $BaZr_{0.2}Ti_{0.8}O_3$ ceramics. *Materials Research Bulletin*. 2014;49:601-607.

12. Liu H, Li Q, Li Y, Luo N, Shim J, Gao J, et al. Structure Evolution and Electrical Properties of $Y^{3+}$-Doped $Ba_{1-x}Ca_xZr_{0.07}Ti_{0.93}O_3$ Ceramics. *Journal of the American Ceramic Society*. 2014;97(7):2076-2081.

13. Rodríguez-Carvajal J. Recent advances in magnetic structure determination by neutron powder diffraction. *Physica B: Condensed Matter*. 1993;192(12):55-69.

14. Roisnel T, Rodríguez-Carvajal J. WinPLOTR: A Windows tool for powder diffraction patterns analysis. *Materials Science Forum*. 2001;378-381:118-123.

15. Mazon T, Hernandes AC, Souza Filho AG, Moraes APA, Ayala AP, Freire PTC, et al. Structural and dielectric properties of $Nd^{3+}$-doped $Ba_{0.77}Ca_{0.23}TiO_3$ ceramics. *Journal of Applied Physics*. 2005;97:104113.

16. Aoujgal A, Ahamdane H, Graça MPF, Costa LC, Tachafine A, Carru JC, et al. Structural and relaxor behavior of $Ba[Zr_xTi_{1-x-y}](Zn_{1/3}Nb_{2/3})_yO_3$ ceramics obtained by a solid-state reaction. *Solid State Communications*. 2010;150(27-28):1245-1248.

17. Samara GA. Pressure and temperature dependences of the dielectric properties of the perovskites $BaTiO_3$ and $SrTiO_3$. *Physical Review*. 1966;151(2):378-386.

18. Outzourhit A, El Idrissi Raghni MA, Hafid ML, Bensamka F, Outzourhit A. Characterization of hydrothermally prepared $BaTi_{1-x}Zr_xO_3$. *Journal of Alloys and Compounds*. 2002;340(1-2):214-219.

19. Moura F, Simões AZ, Paskocimas CA, Zaghete MA, Varela JA, Longo E. Temperature dependence on the electrical properties of $Ba(Ti_{0.90}Zr_{0.10})O_3$:2V ceramics. *Materials Chemistry and Physics*. 2010;123(2-3):772-775.